

Review Article

The use of isotopes in the study of reactions of acyl, phosphoryl, and sulfonyl esters[†]

RICHARD H. HOFF¹ and ALVAN C. HENGGE^{2,*}

¹Department of Chemistry, U.S. Military Academy, West Point, NY 10996, USA

²Department of Chemistry and Biochemistry, Utah State University, Logan, UT 84322-0300, USA

Received 10 May 2007; Accepted 13 June 2007

Abstract: Acyl, phosphoryl, and sulfonyl transfer reactions involving esters and amides are ubiquitous in the biochemical world, and these reactions are found throughout the biochemical pathways involving proteins, nucleic acids, and other compounds essential for life. Such compounds are also common in commercial chemical processes. The use of isotopes has contributed greatly to our understanding of the chemistry of these compounds. There is an enormous body of literature on the use of isotopes in such studies, and this review does not do justice to this great body of knowledge. We cover a selection of reactions for which multiple experimental applications using isotopes have been used in the advancement of mechanistic studies. Copyright © 2007 John Wiley & Sons, Ltd.

Keywords: kinetic isotope effect; solvent isotope effect; ester; amide; phosphate ester; sulfate ester

Introduction

Esters and amides, including phosphate and sulfate esters, are abundant and critical in a host of biological pathways. A broad array of techniques has been used to elucidate the mechanisms by which such compounds are formed and reacted, and these efforts continue, particularly in biological systems.^{1–4} The use of isotopes has played a key role in this effort. This has included the use of isotopes as tracers, in order to follow paths of bond making and breaking, as well as isotope effects, which yield information about the sequence of steps and the nature of transition states. Secondary deuterium isotope effects, and primary and secondary heavy-atom isotope effects, have been crucial to investigations of mechanism and of transition state structure.

Deuterium solvent isotope effects (DSKIEs) have yielded important information in the hydrolysis (and other solvolysis) reactions of esters. A normal solvent

deuterium isotope effect that is larger than about 1.5 is usually interpreted to indicate a proton in flight in the transition state of the rate-limiting step, often the result of a general base mechanism. If this isotope effect is smaller, or slightly inverse, a nucleophilic mechanism is implicated. A particular type of solvent isotope effect experiment, called the proton inventory method, allows for a count of the number of protons contributing to the solvent isotope effect.⁵

There are four heavy atom positions that undergo important bonding changes during reactions of esters. These are central atom (which is carbon, phosphorus, or sulfur in the reactions discussed in this review), the pi-bonded oxygen atom(s), the scissile oxygen atom, and, less often but to a great effect, the nucleophilic atom. The pi-bonded oxygen atoms are also referred to as nonbridging oxygens, and the scissile oxygen will be referred to as the bridging oxygen. The central atom kinetic isotope effect (KIE) has proven to be of limited use in assessing acyl group transfers, and this may prove to be the case also for phosphoryl and sulfonyl group transfers, although there is less data available in the latter two cases. Since both an addition and an elimination step in a mechanism involve considerable reaction coordinate motion on the part of the central atom, a large normal KIE is expected regardless of the step that is rate determining. The collected data for carbonyl-C KIEs for acyl group transfer reactions all

*Correspondence to: Alvan C. Hengge, Department of Chemistry and Biochemistry, Utah State University, Logan, UT 84322-0300, USA. E-mail: hengge@cc.usu.edu

Contract/grant sponsor: NIH; contract/grant number: GM47297
Contract/grant sponsor: PRF; contract/grant number: 35690-AC4

[†]Paper published as part of a special issue on 'Recent Developments in the Use of Isotopically Labelled Molecules in Chemistry and Biochemistry'.

fall in the same narrow range (1.02–1.04).⁶ Because this KIE seems to be insensitive to differences in the mechanism or identity of the rate-limiting step, it is omitted from the discussions that follow. However, isotope effects at the other positions have proven to be highly informative, particularly when multiple isotope effects have been measured on the same reaction. The discussions that follow are limited to reactions for which multiple isotope effects have been obtained.

Isotope effect terminology

Isotope effects are classified as *primary* if a bond to the labeled atom is made or broken during the reaction. Isotope effects measured in other positions are *secondary* isotope effects. A KIE is the ratio of the rate constant of the light isotope to that of the heavy isotope. Similarly, an equilibrium isotope effect (EIE) is a ratio of equilibrium constants. A common notation for isotope effects is to use a leading superscript of the heavier isotope to indicate the isotope effect on the following kinetic quantity; for example, ¹⁵*k* denotes *k*₁₄/*k*₁₅, the nitrogen-15 isotope effect on the rate constant *k*.⁷ An isotope effect is termed *normal* if it is greater than 1, i.e. if the lighter isotopically labeled compound reacts at a faster rate. The isotope effect is *inverse* if this ratio is less than 1. Thus, an isotope effect of unity implies the absence of an isotope effect.

A KIE reflects differences in bonding to the labeled atom in the ground state compared with the transition state of the rate-limiting step. Succinct descriptions of the contributions to isotope effects can be found elsewhere.^{6,8} The essential points are: a primary KIE at an atom undergoing bond cleavage will be normal, due to the preference of the heavier isotope for the lower energy (more tightly bonded) position; secondary KIEs are inverse if the labeled atom becomes more tightly bonded in the transition state, and normal if bonding becomes looser. Similarly, EIEs are determined by differences in ground state bonding, and both inverse and normal EIEs are common.⁹

KIEs can be measured by either the *direct* or the *competitive* method. In the direct method, the individual rate constants for the two isotopically labeled species are measured. This approach works well for deuterium isotope effects since these are usually large. However, the rate difference resulting from isotopic substitution at carbon, nitrogen, or oxygen is never more than about 8%. Hence, the competitive method is usually the method of choice for the measurement of heavy-atom (atoms heavier than hydrogen) isotope effects. In this method, a mixture of the light and heavy isotopic isomers is allowed to react competitively, and the isotope effect is measured from the change in

isotopic composition over the course of the reaction. A high degree of precision is desirable in the isotope ratio measurements. Several methods have been utilized.¹⁰ An isotope ratio mass spectrometer (IRMS) is the most precise way of obtaining these ratios, but has the drawback of requiring that the atom of interest be amenable to quantitative transformation into one of the small molecule gases (CO or CO₂ for carbon or oxygen, N₂, SO₂ for sulfur) that these instruments are designed to analyze. The remote label method considerably expands the ability to use the IRMS technology to measure isotope effects.^{11,12} In this method, an atom that is easily isolated is incorporated as a reporter into the molecule under study. Two isotopic isomers of the compound are prepared, one with the light isomer in the position of interest and in the reporter position, and the other with the corresponding heavy isotopes. These are then mixed, usually in a ratio that reconstitutes close to the natural abundance of the reporter atom. The isotope ratios in the product and residual substrate after partial reaction are then measured in the reporter atom, and after correction for any isotope effect from the isotopic substitution in the reporter position itself, and for levels of isotopic incorporation, the isotope effect at the position of interest is obtained.

Acyl transfer reactions

Esters

Acyl transfer reactions involve nucleophilic attack on the carboxylic acid functional group and its major derivatives (acid halides, anhydrides, esters, and amides). Their biochemical relevance has made this one of the most studied classes of reactions in chemistry.¹ One of the best known use of isotopes was the use of ¹⁸O as a tracer in hydrolysis reactions to identify the location of bond fission¹³ and to provide the first direct evidence for the existence of tetrahedral intermediates.¹⁴ The exchange of ¹⁸O between water and the oxygen atom of the carbonyl group in unhydrolyzed ester (a positional isotope exchange, or PIX, experiment) implied the existence of a tetrahedral intermediate, which at the time was only a subject of conjecture. Recent physical organic investigations suggest that esters with good (i.e. aryloxy) leaving groups undergo acyl transfer by a concerted mechanism with no intermediate, which will be described below. Still a third pathway, the acylium ion mechanism followed by acyl halides, is well known, giving a rich variety of mechanisms available to acyl transfer chemistry.¹⁵

The PIX experiment described above provides the partition ratio of the tetrahedral intermediate (defined as the ratio of the forward, or hydrolysis, pathway relative to proton equilibration and reversion to the reactant ester, or $k_{\text{hydrolysis}}/k_{\text{exchange}}$), assuming that the protonic equilibration of the intermediate is rapid. In Scheme 1A, this means that equilibration of the proton between the oxygen atoms in -OH and -O^- must be much faster than in either k_{-1} or k_2 . A direct test of this assumption was carried out for the base-catalyzed hydrolysis of ethyl and isopropyl toluate. If rapid proton equilibration does not occur, then the proton transfer should be at least partially rate limiting on the exchange, resulting in a significant DSKIE on the exchange rate. The DSKIEs for k_{exchange} during the base hydrolysis of ethyl and isopropyl toluate were found to be 0.97 and 0.86, respectively, consistent with rapid protonic equilibration.¹⁶

Multiple KIEs have been measured for the alkaline hydrolysis of methyl benzoate¹² and methyl formate,¹⁷ and all data point to a stepwise mechanism involving tetrahedral intermediates. PIX experiments give partition ratios of ~ 18 to 30. These results indicate that the attack of hydroxide is largely rate determining. The nature of the transition state has been studied by a number of primary and secondary KIE investigations. The alpha-secondary KIE ($^Dk_{\text{formyl}}$) for methyl formate (where $R = \text{H/D}$ in Scheme 1) is small and inverse (0.95).¹⁸ This secondary KIE is sensitive to hybridization changes at the carbonyl carbon. An inverse KIE results when the carbon atom is transformed from an sp^2 -hybridized ground state toward tetrahedral sp^3 -hybridization in the transition state. The magnitude of the KIE reflects the degree of hybridization change, with a maximum inverse KIE expected to be near 0.75.¹⁹

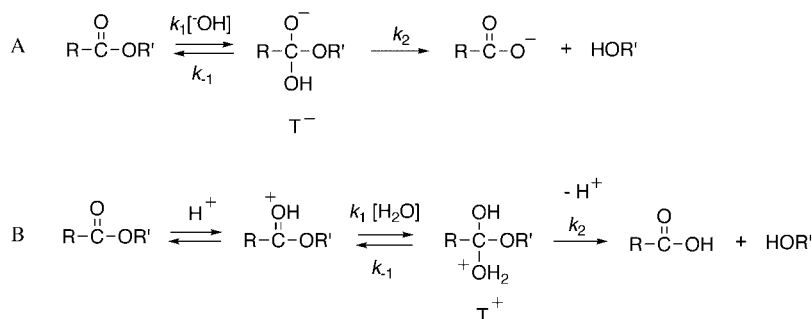
The conclusions of the PIX experiments (i.e. rate-determining first step), together with the small $^Dk_{\text{formyl}}$, point to an early sp^2 -like transition state. The $^{18}k_{\text{bridge}}$ KIEs are small (1.009 for methyl formate¹⁷ and 1.006 for methyl benzoate¹²), consistent with a mostly

rate-determining first step. The small normal KIEs were attributed to a small contribution from step 2 of the mechanism, and from the weakening of the bond to leaving oxygen resulting from the tetrahedral intermediate formation. The measurement of the nucleophile ^{18}O KIE was particularly revealing and indicated that the most likely nucleophile is not hydroxide directly, but rather one of the water molecules solvating the hydroxide ion.²⁰ Jencks reached a similar conclusion from the observation of general base catalysis in the hydrolysis of formate esters.²¹

The acid hydrolysis of esters involves protonation of the carbonyl oxygen atom, followed by addition of water and breakdown of the tetrahedral intermediate to product (Scheme 1B). The partition ratio for methyl formate¹⁷ from PIX experiments is smaller than for the alkaline hydrolysis but still favors hydrolysis ($k_{\text{h}}/k_{\text{e}} = 11.4$), consistent with the rate-determining formation of T^+ .

The $^Dk_{\text{formyl}}$ for the acid-catalyzed hydrolysis of methyl formate is more inverse (0.81)¹⁸ indicating considerable sp^3 character in the transition state. The $^{18}k_{\text{bridge}}$ values are small for both methyl formate (1.0009)¹⁷ and methyl benzoate (1.002),²² indicating rate-limiting formation of the tetrahedral intermediate. The $^{18}k_{\text{carbonyl}}$ for the acid-catalyzed hydrolysis of methyl benzoate (0.995)²² is inverse, whereas the corresponding $^{18}k_{\text{carbonyl}}$ for the alkaline hydrolysis is normal (1.005). The net inverse value probably reflects the inverse effect from protonation offsetting the normal effect from the partial loss of the pi bond.

The hydrazinolysis of esters exhibits a break in the $\log k$ vs pH profile, indicating a change in the rate-determining step with pH. This was proposed²³ to result from a change in the rate-determining step from breakdown of an anionic tetrahedral intermediate at low pH, to the general base-catalyzed formation of this intermediate at high pH. Isotope effects have been measured for the hydrazinolysis of both methyl benzoate and methyl formate.^{12,17,18,24} The methyl formate KIE data are the most revealing, since they have been



Scheme 1

obtained at both low and high pH. At pH 8, a small $^Dk_{\text{formyl}}$ (0.98)¹⁸ indicates a transition state with nearly the same hybridization as the ground state. The large $^{18}k_{\text{bridge}}$ (1.062)¹⁷ indicates considerable C–O bond fission in the transition state of the rate-determining breakdown of the tetrahedral intermediate. Evidently this transition state is late, with the carbonyl carbon returned nearly to sp^2 hybridization and the pi bond largely re-formed. The observation of an inverse nucleophile KIE ($^{15}k_{\text{nuc}} = 0.990$)²⁴ indicates that the bond to the nucleophile has formed before the rate-determining step, since bond formation during the rate-determining step should result in a normal $^{15}k_{\text{nuc}}$. If breakdown of the tetrahedral intermediate is rate limiting, this KIE will have no imaginary frequency factor and will essentially be an EIE.

At pH 10, $^Dk_{\text{formyl}}$ is more inverse (0.76)¹⁸ and consistent with a more sp^3 -like transition state. The magnitude of $^{18}k_{\text{bridge}}$ is reduced to 1.005,¹⁷ suggesting that the formation of the tetrahedral intermediate is rate determining. These results are consistent with a change in the rate-determining step at pH 10.

For esters with good (aryloxy) leaving groups, linear free energy relationships²⁵ and calculations^{26,27} offer evidence for a concerted acyl transfer mechanism with no intermediate. This proposal is not universally accepted, and structure–activity data obtained using other approaches have been offered as indicative of the usual tetrahedral mechanism for such esters.²⁸ KIEs have been measured for the alkaline hydrolysis reaction of *p*-nitrophenyl acetate (*p*NPA), and for the acyl transfer with a number of nucleophiles having a pK_a from 9.3 to 9.9. The leaving group *p*-nitrophenol has a pK_a of 7.14, and as a result, if a tetrahedral intermediate forms it should partition forward a majority of the time ($k_2 \gg k_{-1}$ in Scheme 1A). In other words, formation of the intermediate will be rate limiting. The most diagnostic isotope effects are the β -deuterium and the $^{18}k_{\text{bridge}}$ KIEs. The β -deuterium KIE, measured with three deuterium atoms in the acetyl methyl group, is a secondary one; it arises from changes in hyperconjugation, which arise from hybridization changes at the carbonyl carbon atom.²⁹ With oxyanion or sulfur anion nucleophiles, a small inverse β - Dk is observed (from 0.95 to 0.98); the expected maximum for a fully sp^3 -hybridized transition state is about β - $^Dk = 0.89$.³⁰ Therefore, no significant rehybridization occurs in the transition states for these reactions, consistent with either a concerted mechanism or a very early transition state for the formation of a tetrahedral intermediate. The $^{18}k_{\text{bridge}}$ provides strong evidence for the concerted pathway. The significant magnitude of these KIEs (1.0135–1.0219; the maximum value is ~ 1.03)³⁰ indicates significant C–O bond fission to the leaving

group in the transition state. These values are much larger than the $^{18}k_{\text{bridge}}$ KIEs in the alkaline hydrolysis of methyl formate (1.009) and methyl benzoate (1.006), where the formation of T^- is rate determining. A stepwise mechanism with *p*NPA should show leaving group KIEs even smaller than these, since the superior leaving group in *p*NPA should make tetrahedral intermediate formation even more rate limiting. Thus, the large observed $^{18}k_{\text{bridge}}$ KIEs strongly support the concerted mechanism for most reactions of *p*NPA. A recent computational study of the alkaline hydrolysis of *p*NPA using density functional theory found that the solvent plays a crucial role in affecting the concertedness of the reaction and yielded calculated KIEs in good agreement with the experimental ones.²⁷

The aminolysis of *p*NPA was also examined and is the only exception. A large $^{18}k_{\text{bridge}}$ (1.033) indicates near complete fission of this bond in the transition state. This is consistent with either a concerted mechanism or a rate-limiting breakdown of a tetrahedral intermediate; such a partitioning pathway was ruled out for the other nucleophiles used. However, in the aminolysis reaction, the initially formed tetrahedral intermediate is zwitterionic, with a positively charged nitrogen, which is an even better leaving group than *p*-nitrophenolate. The large $^{18}k_{\text{bridge}}$ in the aminolysis of *p*NPA recalls those observed for hydrazinolysis of methyl formate and methyl benzoate at pH 8, where breakdown of T^- is rate determining. The small β - Dk (0.968) indicates close to sp^2 hybridization in the transition state. The KIEs for *p*NPA aminolysis are consistent with either the concerted mechanism seen with anionic nucleophiles or a very late transition state for breakdown of an intermediate.

The enzymatic reactions of *p*NPA with chymotrypsin, carbonic anhydrase, papain, and acid protease were also examined.³¹ The KIEs were similar to those measured for the uncatalyzed aqueous reactions, but with less inverse values for β - Dk . This is attributed to greater hydrogen bonding or other electrostatic interaction with the ester carbonyl oxygen atom in the transition state. Such an interaction would maintain more of the hyperconjugation present in the ground state that would normally be lost by partial hybridization changes upon nucleophilic attack.³¹

Amides

Although much less reactive than esters, amides undergo hydrolysis at acidic, basic, or neutral pH. The kinetics of the alkaline hydrolysis for most amides is generally first order in hydroxide at low base concentrations; for more highly reactive amides, the reaction is second order in hydroxide under strongly

alkaline conditions.³² The proposed mechanism involves the formation of two tetrahedral intermediates (Scheme 2). The first, T^- , is formed upon attack of hydroxide; its subsequent deprotonation by a second molecule of hydroxide results in the formation of the second, T^{2-} .

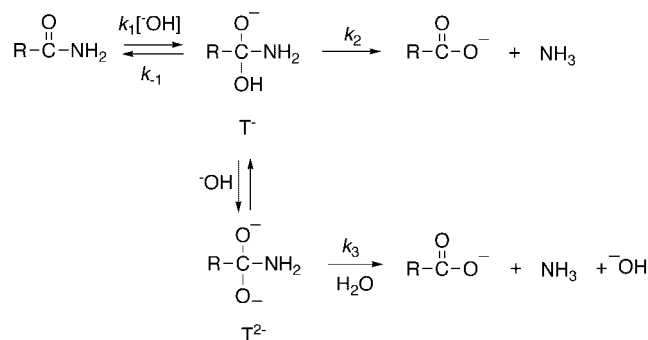
In PIX experiments with formamide, k_h/k_e was shown to be dependent on hydroxide concentration.³³ Under dilute alkaline conditions, hydrolysis and exchange occur at similar rates ($k_h/k_e = 1.05$). At higher pH, more of the intermediate is trapped as T^{2-} , which reduces exchange and favors hydrolysis. PIX experiments show that the exchange does not accompany the water reactions of two amides with more activated leaving groups, *p*-nitrotrifluoroacetanilide, and trifluoroacetanilide.³⁴ Proton inventory data imply the involvement of at least two water molecules in the transition state. The data support a water reaction involving the rate-limiting formation of a neutral tetrahedral intermediate, which preferentially undergoes C–N fission in preference to reversion to amide with exchange.

The alkaline hydrolysis of formamide³³ has been the subject to a number of isotope effect studies. Kirsch found the magnitude of $^Dk_{\text{formyl}}$ ($R = \text{H}$ or D in Scheme 2) to be dependent on the concentration of hydroxide, consistent with a pH-dependent mechanism. The $^{15}k_{\text{bridge}}$ (1.004) seems smaller than that expected under conditions where C–N bond fission should be rate limiting; however, C–N bond fission probably requires the nitrogen to be protonated, which will contribute an inverse effect to the overall observed $^{15}k_{\text{bridge}}$. Marlier's measured nucleophile, $^{18}k_{\text{nuc}}$, of 1.022 indicated that, as in the case of ester hydrolysis, the nucleophile is one of the water molecules solvating the hydroxide ion.²⁰ In a subsequent investigation of whether hydroxide acts as a nucleophile or a general base, Brown measured the solvent deuterium KIEs and proton inventory.³⁵ An inverse solvent DSKIE of 0.77 was found, and proton inventory data were consistent

with either mechanism. In order to accommodate the inverse DSKIE, which rules out a proton transfer in the rate-limiting step, and the $^{18}k_{\text{nuc}}$, a mechanism was proposed involving an encounter complex between formamide and solvated hydroxide in which the carbonyl carbon is exposed to a lone pair of electrons in one of the solvating waters. Proton transfer, exposing the carbonyl to a 'hot hydroxide' molecule that immediately attacks, then follows. The major difference between this mechanism and that proposed by Marlier is in the timing of the proton transfer.

The variation in β -deuterium isotope effects with pH on the alkaline hydrolysis of *p*-nitroacetanilide (*p*NAA) led to the conclusion that at 0.002 N $[\text{HO}^-]$ ($\beta\text{-}^Dk = 0.967$), decomposition of a tetrahedral adduct formed by the addition of hydroxide to *p*NAA is rate determining, while at 2 N $[\text{HO}^-]$ ($\beta\text{-}^Dk = 0.933$), nucleophilic attack by hydroxide is rate determining.³⁶ Similar conclusions resulted from measurements of the DSKIE on the hydrolysis of formamide at 0.075 N $[\text{LO}^-]$ (DSKIE = 1.15) and at 1.47 N $[\text{LO}^-]$ (DSKIE = 0.77). The inverse value under the more basic conditions was interpreted to imply the rate-limiting nucleophilic attack.³⁷

Subsequently, the ^{15}N -isotope effects were measured; at 0.002 N $[\text{HO}^-]$, $^{15}k_{\text{amido}} = 1.035$, whereas at 2 N $[\text{HO}^-]$, $^{15}k = 0.995$.³⁸ The large normal effect of 1.035 at $[\text{HO}^-] = 0.002$ N reflects the rate-limiting decomposition of the tetrahedral intermediate and results primarily from C–N bond fission. The value is close to the theoretical maximum of 1.044 that has been calculated for breaking a C–N bond.³⁹ The ^{15}N and $\beta\text{-}^Dk$ KIEs indicate a late transition state in which the hybridization of the carbonyl carbon atom has returned to nearly sp^2 and the pi bond is largely reformed. In contrast, at 2 N $[\text{HO}^-]$ the small inverse $^{15}k_{\text{amido}}$ reflects the rate-limiting intermediate formation. This KIE most likely results from the hybridization change of the carbonyl carbon from sp^2 toward sp^3 . For this step, $^{15}k_{\text{amido}}$ is a secondary KIE adjacent to the



Scheme 2

carbon atom undergoing a change in hybridization and is predicted to be inverse due to the compression of bending modes.⁴⁰ Apparently, this effect is more pronounced than the reduction in C–N bond order from loss of amide resonance, since the latter would result in a normal isotope effect.

Phosphoryl transfer reactions

Substitution reactions of tetrahedral phosphate esters can occur by three limiting mechanisms: a dissociative S_N1-type mechanism, designated D_N + A_N in the IUPAC nomenclature; an addition–elimination mechanism (A_N + D_N); and a concerted mechanism (A_ND_N) with no intermediate (Figure 1). In the D_N + A_N mechanism, a metaphosphate-like intermediate is formed, whereas in the A_N + D_N mechanism a pentacoordinate phosphorane is formed. In the concerted mechanism, there is

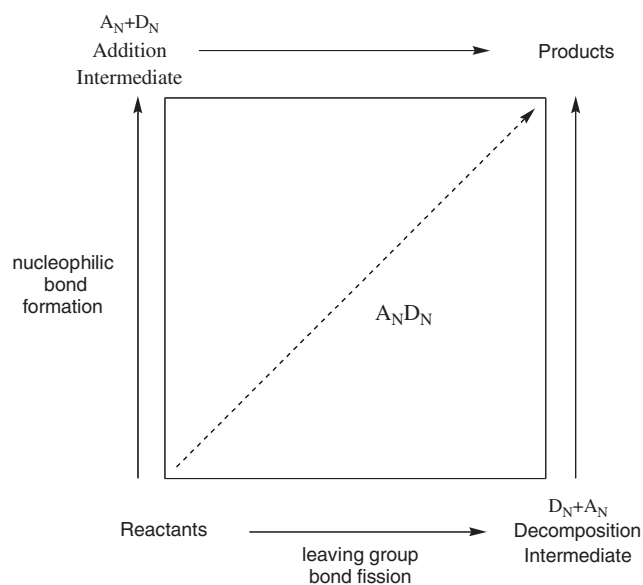


Figure 1 A More-O'Ferrall-Jencks diagram illustrating the mechanistic possibilities open to carboxyl, phosphoryl, and sulfonyl esters. Stepwise mechanisms follow one of the pathways around the perimeter, whereas a concerted mechanism will have a transition state that may lie anywhere in the interior.

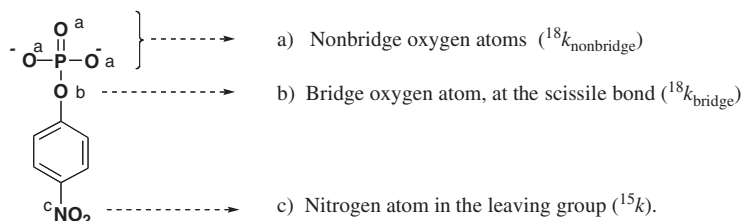


Figure 2 The locations of KIE measurements for reactions of pNPP.

simultaneous bond formation to the nucleophile and fission of the bond to the leaving group. This transition state could have a range of associative or dissociative character depending on the synchronicity between bond fission and bond formation.

The development of substrates that are chiral at the phosphorus atom provided a useful tool in the study of phosphoryl transfer. This has been accomplished by the use of oxygen isotopes⁴¹ and through the use of one sulfur atom and two oxygen isotopes.⁴² A free metaphosphate (or thiometaphosphate) intermediate from a chiral substrate reveals itself by the formation of racemized product. In enzymatic reactions, a direct in-line transfer will result in inversion; a phosphoenzyme intermediate results in a product with retention of stereochemistry. The stereochemical outcomes of a number of enzyme-catalyzed reactions have been determined using these methods.²

Monoesters

Phosphate monoesters at physiologically relevant pH exist as either the monoanionic or dianionic species. A large body of evidence indicates that both of these species undergo phosphoryl transfer via a dissociative pathway characterized by a metaphosphate-like transferring phosphoryl group.³ The near complete bond cleavage to the leaving group is supported by large values of β_{lg}, the modest participation of the nucleophile by small Brønsted β_{nuc} values, and the dissociative character by the near zero entropies of activation.⁴³ In spite of the highly dissociative nature of the transition state, free metaphosphate is not formed in protic solvents.⁴⁴ The monoanionic species generally react at higher rates than the dianions. The β_{lg} is reduced compared with that of the dianion, evidence of a proton transfer to the leaving group more or less synchronized with bond cleavage.

Measurements of KIEs on phosphoryl transfer from monoesters are in agreement with conclusions from LFER experiments. Most of the KIEs on phosphoryl transfer have been obtained using *p*-nitrophenyl phosphate (pNPP), with KIEs measured at the positions

shown in Figure 2. The $^{18}k_{\text{bridge}}$ is a primary isotope effect and measures bond fission to the leaving group, while $^{18}k_{\text{nonbridge}}$ and ^{15}k are secondary. The nonbridge KIE is normal for the formation of phosphorane intermediates due to loss of the P–O pi bond and is very small and inverse in a metaphosphate-like transition state. Delocalization of negative charge in the leaving group results in small normal values of ^{15}k , up to a maximum of about 1.003.⁴⁵

The ^{15}k KIE is much larger in the hydrolysis of the *p*NPP dianion (1.0034) than in the monoanion (1.0005). This is consistent with the synchronous protonation of the leaving group in the latter reaction. The $^{18}k_{\text{bridge}}$ is a primary isotope effect; hence, it should be the most pronounced. For aqueous hydrolysis a large (1.023) normal effect was found, indicating advanced fission of the bond to the leaving group in the transition state.^{46,47} The $^{18}k_{\text{nonbridge}}$ KIE in the *p*NPP dianion hydrolysis is small and inverse (0.9993), indicating little change in bond order to the phosphorus. During hydrolysis of the monoanion, this KIE becomes large and normal (1.022), which is attributed to deprotonation.⁴⁷

Diesters

The reaction rates of diesters are sensitive to both the leaving group and the nucleophile, which is a qualitative evidence of a concerted mechanism. The β_{lg} is lower than that for the monoester, while the β_{nuc} is higher.^{48,49} Together, compared with monoester reactions, these data indicate a tighter transition state, with the bond to the nucleophile more developed and less cleavage of the bond to the leaving group.

The KIE data for diester hydrolysis reactions are consistent with the concerted mechanism implied by the LFER studies. The $^{18}k_{\text{bridge}}$ for several diesters with *p*-nitrophenol as the leaving group are in the range of 1.004–1.006.⁵⁰ In addition, the nucleophile ^{18}O KIE for the attack of hydroxide on thymidine-5'-*p*NPP was found to be 1.027.⁵¹ This large normal isotope effect is evidence for direct attack by hydroxide in the rate-limiting step and significant bond formation in the transition state. These two isotope effects, combined with the earlier studies, suggest a tighter transition state than in the monoesters, with greater

nucleophile participation and less bond fission to the leaving group.

Triesters

The kinetic stability of monoesters and diesters is largely based on their negative charge, which repels nucleophiles. Thus, it is not surprising that the neutral triesters are the most reactive of the series. A number of mechanistic studies including stereochemical analyses have been carried out on 6-member ring cyclic triesters (Figure 3). An LFER study measured β_{lg} values between –0.4 and –0.88 depending on the basicity of the nucleophile.⁴⁸ As the nucleophile strength increased, the leaving group dependency decreased. The favored interpretation of this was that the mechanism involves a two-step process and a phosphorane intermediate. However, the stereochemistry of the reaction was found to vary between inversion and retention based on many factors including solvent, counterions, and substitution.⁵² This could result from pseudo-rotation of phosphorane intermediates, or from competing concerted and $A_{\text{N}} + D_{\text{N}}$ mechanisms.

In KIE studies of a series of acyclic diethyl phosphate triesters with different leaving groups, the most striking results are the nonbridge ^{18}O isotope effects. While $^{18}k_{\text{nonbridge}}$ showed little change in the bond order of the nonbridge oxygens in mono and diesters, $^{18}k_{\text{nonbridge}}$ values on triester reactions vary from a low of 1.006 with the *p*-nitrophenyl leaving group to a high of 1.033 for the choline iodide leaving group.⁵³ For perspective, the calculated isotope effect is 1.040 for the change in bond order from double to single bond for the phosphoryl oxygen.⁵³ While this points to an increasingly associative transition state as leaving group basicity increases, it does not rule out a two-step mechanism. Unexpectedly, the primary isotope effect also increases, from 1.006 when the leaving group is *p*-nitrophenyl to 1.052 for *m*-nitrobenzyl. This cannot be explained without involving the imaginary frequency factor contribution to the isotope effect.⁵³

In summary, the transition states for the series of phosphate monoester, diester, and triester phosphoryl transfer reactions show signs of concerted nucleophilic attack and leaving group bond fission. The looseness

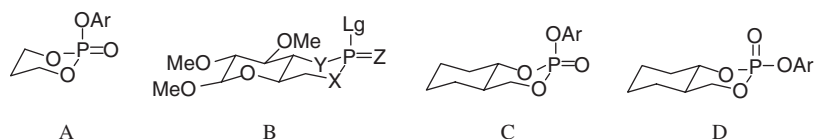


Figure 3 Some of the 6-membered cyclic phosphotriesters used for mechanistic studies cited in the text. In structure B, Lg designates the leaving group, Z was oxygen or sulfur, and X and Y were either oxygen, sulfur, or *N*-methyl.^{48,52}

of the transition state in the monoester lies closest to the free metaphosphate extreme (the lower right corner of Figure 1), whereas the transition state for triester hydrolysis resembles a pentacoordinate phosphorane. All three phosphate esters feature an emerging single negative charge on the transition state; the monoester dianion by shedding a negative ion in the leaving group, the diester by maintaining a relatively synchronous transition state with a unit charge, and the triester by shifting the negative charge from the nucleophile to the phosphoryl oxygen.

Enzymatic phosphoryl transfer

Alkaline phosphatase

Alkaline phosphatase (AP) is one of the most extensively studied phosphatases and is a two-metal catalyst. The catalyzed reaction proceeds via an intermediate in which a serine residue is phosphorylated, which is subsequently hydrolyzed. The active site of the enzyme contains two zinc ions directly involved in catalysis (Figure 4). While a nonbridge oxygen coordinates with both zinc ions, one (Zn1) stabilizes the negative charge on the ester oxygen of the leaving group while the other (Zn2) coordinates with the serine oxygen to facilitate its deprotonation. Once the intermediate is formed, Zn1 then coordinates with a water molecule, creating a hydroxyl nucleophile that displaces the phosphate from serine.

Attempts to study this reaction were restricted because a nonchemical step, such as binding or a conformational change, is rate limiting on $k_{\text{cat}}/K_{\text{m}}$ with aryloxy ester substrates. A recent series of experiments used a sulfate monoester substrate with wild-type AP and a phosphate monoester with a mutant R166S AP to overcome this limitation.⁵⁴ The kinetic data and KIEs indicate a key role in catalysis for the interaction of a charged nonbridge oxygen with the metal ions. The comparison of $^{18}(\text{V}/\text{K})_{\text{bridge}}$ with the $^{18}k_{\text{bridge}}$ for the

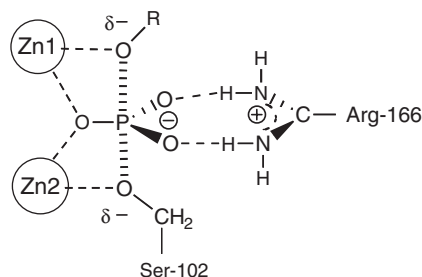


Figure 4 A schematic diagram of the bonding changes in the transition state of the reaction catalyzed by alkaline phosphatase, based on X-ray structures, LFER, and KIE data.

uncatalyzed hydrolysis shows a decrease in the isotope effect to 1.01 from roughly 1.02, respectively. This decrease is similar to the decrease caused by protonation of the leaving group and is attributed to a strong transition state interaction of the leaving group with Zn1. The nonbridge isotope effects are significantly more inverse for the AP-catalyzed reaction: 0.994 for $^{18}k_{\text{nonbridge}}$ vs 0.909 $^{18}(\text{V}/\text{K})_{\text{nonbridge}}$ in the AP-reaction. This suggests a strong interaction between the negatively charged oxygen and the metals, such that vibrational modes are stiffened. When these experiments were repeated with the sulfate substrate, *p*-nitrophenyl sulfate (*p*NPS), the $^{18}(\text{V}/\text{K})_{\text{bridge}}$ showed the same reduction compared with the value in the uncatalyzed hydrolysis, but the $^{18}(\text{V}/\text{K})_{\text{nonbridge}}$ was identical to the uncatalyzed result. The enzyme is a much better catalyst (by a factor of 10^9) for phosphate monoesters over sulfate monoesters. The KIE data support the idea that the catalytic proficiency of AP is based on the interaction with negative charge on the substrate, and that the active site has evolved to preferentially recognize the phosphoryl group over the sulfuranyl group.

Protein tyrosine phosphatases

The protein tyrosine phosphatases (PTPases) share a common signature motif with essential cysteine and arginine residues in the active site and share the ability to dephosphorylate peptides containing a phosphotyrosine, and small molecule aryloxy phosphate esters, via a phosphocysteine intermediate.⁵⁵ These enzymes have been subjected to intense study and the functions of

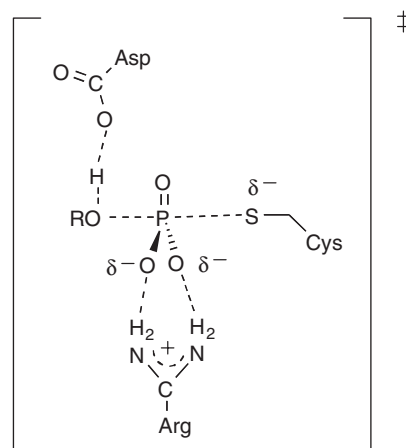


Figure 5 The transition state for the native PTPase-catalyzed phosphoryl transfer from substrate to enzyme. P–O bond fission and protonation of the leaving group are both far advanced, and nucleophilic participation is small in the loose transition state.

the individual residues are well understood. The cysteine must be deprotonated for catalysis, and the neighboring residues assist in lowering its pK_a , maintaining it in the thiolate form. A conserved aspartic acid serves as a general acid to protonate the leaving group in the first step, then as a general base to promote attack by water in the hydrolysis of the phosphocysteine intermediate. This residue resides on a flexible loop that closes on the active site when triggered by oxyanion binding.⁵⁶

KIE studies have been conducted using *p*NPP to probe the transition state of the first phosphoryl transfer step, the formation of the phosphoserine intermediate, with the *Yersinia* PTP and PTP1,⁵⁷ VHR,⁵⁸ and Stp1.⁵⁹ For each of these PTPases, the $^{18}(V/K)_{\text{nonbridge}}$ is negligible (0.9998–1.0003), mirroring the results for uncatalyzed monoesters and suggesting that the transition state is loose (Figure 5). The values for $^{15}(V/K)$ are near unity for all PTPases except Stp1. This implies that the protonation of the leaving group is synchronous with P–O bond fission. With Stp1, a small normal $^{15}(V/K)$ of 1.0007 indicates partial charge on the leaving group in the transition state. The range of $^{18}(V/K)_{\text{bridge}}$ values for all four enzymes (1.0118–1.0171) is consistent with a late transition state, with fission of the P–O bond well advanced accompanying the protonation of the leaving group. When the general acid Asp is mutated to Asn, the isotope effects in all of the PTPases show a shift to more nucleophilic participation, and essentially a full negative charge on the leaving group which now departs as the unprotonated anion: $^{15}(V/K) = 1.0024\text{--}1.0030$, $^{18}(V/K)_{\text{bridge}} = 1.0275\text{--}1.0295$, and $^{18}(V/K)_{\text{nonbridge}} = 1.0019\text{--}1.0024$.

Calcineurin

Calcineurin (PP2B) is a member of the serine/threonine phosphatase family.⁶⁰ Members of this family utilize a binuclear metal center to hydrolyze phosphate monoesters (Figure 6). KIEs were studied using *p*NPP as a substrate.⁶¹ Calcineurin poses a problem in that a nonchemical step is partially rate limiting at the pH optimum; by noting isotope effects at both this pH and at a pH which reduces the commitment factor, the intrinsic isotope effect can be estimated. From the $^{15}(V/K)$ of 1.0014 at nonoptimum pH, it is implied that the leaving group has a partial negative charge in the transition state, consistent with the Brønsted β_{lg} of -0.3 .⁶² Calcineurin has a histidine residue in a position that might allow it to function as a general acid to protonate the leaving group. Taken together, it appears that the putative proton transfer lags P–O bond fission in the transition state. The $^{18}(V/K)_{\text{bridge}}$

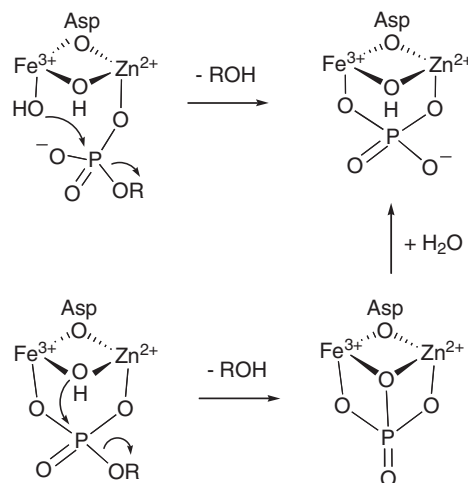


Figure 6 Two possible binding modes and mechanisms for catalysis by the metal centers in calcineurin and lambda phosphatases, and by related bimetallophosphatases. In calcineurin, the metals *in vivo* are believed to be Fe^{3+} and Zn^{2+} . In lambda, the metals *in vivo* are uncertain, and Mn^{2+} is used in most kinetic studies.

goes from 1.007 at optimum pH to 1.015 off optimum, implying an intrinsic value which approaches that of the uncatalyzed hydrolysis. The $^{18}(V/K)_{\text{nonbridge}}$ (0.9942) is small but more inverse than for uncatalyzed hydrolysis, possibly due to interaction with the metal ions at the active site, recalling the change noted with AP described above. The overall picture that emerges is of a loose transition state with significant bond fission to the leaving group.

Lambda protein phosphatase

KIEs have also been measured for the hydrolysis of *p*NPP catalyzed by the related lambda protein phosphatase (λ PP).⁶³ Experiments confirmed that the chemical step of phosphoryl transfer was fully rate limiting with this enzyme and the intrinsic isotope effects were observed. A $^{15}(V/K)$ of 1.0006–1.0007 with the native enzyme shows very small negative charge on the leaving group. This increases to 1.0016 when the putative general acid histidine is mutated to asparagine. This increase is less than that expected if the leaving group is fully negatively charged, implying that some other electrophilic entity stabilizes the leaving group, either a metal-coordinated water or one of the metal ions. The $^{18}(V/K)_{\text{bridge}}$ results (1.013–1.014) are close to those of the PTPases, where there is a significant bond fission in the transition state. The $^{18}(V/K)_{\text{bridge}}$ (0.9976–0.9992) is consistent with the values observed for the uncatalyzed dianion substrate, which has a loose transition state.

Phosphotriesterase

Phosphotriesterases are much less common in the biosphere, as there are no known naturally occurring phosphotriesters. These enzymes have apparently evolved in response to the human introduction of such compounds into the environment.⁶⁴ The phosphotriesterase from the soil bacterium *Pseudomonas diminuta*, the best characterized member of this family, has two zinc ions in the active site, with a bridging hydroxyl between the ions postulated as the nucleophile (Figure 7).⁶⁵ An X-ray structure obtained with a bound nonhydrolyzable substrate analogue, and modeling studies, suggests a binding mode with the bridging hydroxide positioned opposite the leaving group. The stereochemistry of the reaction results in inversion of configuration at phosphorus.⁶⁶ An LFER study found that the β_{nuc} was high (-1.8) for poor leaving groups ($\text{p}K_{\text{a}} > 7$) indicating rate-limiting phosphoryl transfer, but low for good leaving groups.⁶⁷ The KIEs measured with the substrates paraoxon ($^{18}(\text{V}/\text{K})_{\text{bridge}} = 1.0020$ and $^{18}(\text{V}/\text{K})_{\text{nonbridge}} = 1.0021$) and diethyl 4-carbamoylphenyl phosphate ($^{18}(\text{V}/\text{K})_{\text{bridge}} = 1.036$ and $^{18}(\text{V}/\text{K})_{\text{nonbridge}} = 1.0181$) reflected the less rate-limiting chemistry with paraoxon.⁶⁸

The solvent isotope effects were measured to examine the kinetic significance of the proton transfer steps in the mechanism. The small isotope effect (< 2.0) suggests that proton transfer is not involved in the rate-limiting step and probably follows P–O bond fission. The overall conclusion from the LFER and KIE data indicates a concerted mechanism with nucleophilic attack by the bridging hydroxide to produce a transition state with leaving group bond fission nearly complete. The leaving group bears a nearly complete

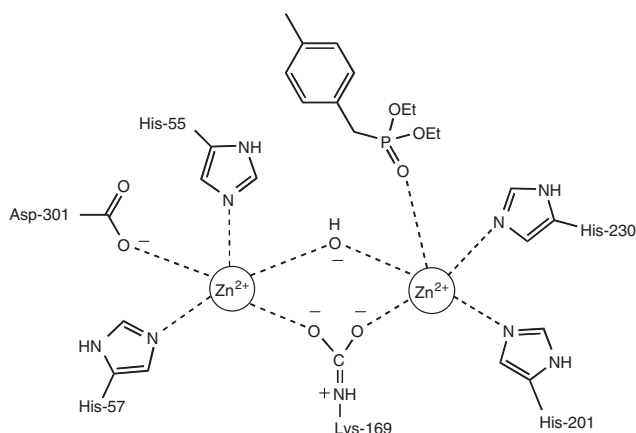


Figure 7 The structure of the active site of the phosphotriesterase from *Pseudomonas diminuta*, with a bound substrate analogue.⁶⁵

negative charge, without stabilization by enzymatic interactions.

Sulfate esters

While not as biochemically ubiquitous as phosphoryl transfer reactions, sulfonyl (SO_3^-) transfer is also a frequently observed mechanism for signaling and regulation.

Sulfate monoesters. Isotope tracer studies in ^{18}O -labeled water show that aryloxy sulfates undergo S–O bond fission in the pH-independent region, whereas both alkyl and aryloxy sulfates react by C–O fission above pH 13.^{69,70} LFER studies of sulfate monoester reactions in the pH-independent region found Brønsted $\beta_{\text{lg}} (-1.2)$ ⁷¹ and $\beta_{\text{nuc}} (0.20)$ ⁶⁹ values very close to those of phosphate monoesters. These values suggest a transition state with advanced leaving group bond fission and little nucleophilic participation, in which the sulfonyl group resembles sulfur trioxide (Figure 8(A)). The possibility of a completely dissociative two-step mechanism was ruled out by a stereochemical study using phenyl sulfate made chiral using oxygen isotopes, which found that the reaction proceeds by inversion.⁷²

The KIEs for the hydrolysis of *p*NPS were measured for the anionic form and under acidic conditions, where the reactive species is the neutral molecule. For the anion reaction, the ^{15}k of 1.0026 and $^{18}k_{\text{bridge}}$ of 1.021 indicate that virtually a full negative charge resides on the leaving group in the transition state, and that the O–S bond is largely broken. The $^{18}k_{\text{nonbridge}}$ (0.9951) is more inverse than seen with phosphomonoesters. This clearly suggests an increase in the bond order between the nonbridge oxygens and sulfur, supportive of the sulfur trioxide-like transition state.

Even in 10 N HCl, the sulfate monoester is less than 0.01% protonated (the estimated $\text{p}K_{\text{a}}$ is -5). Still, under these conditions, the β_{lg} was reduced to -0.22 ⁷¹ and a solvent isotope effect of 2.43 in which observed.⁷³ This led to a proposal of a two-step mechanism for the neutral sulfate monoester in which proton transfer to the leaving group is followed by O–S bond cleavage (Figure 8(B)). This was supported by KIE studies which found ^{15}k reduced to nearly unity under these conditions.⁷⁴ The $^{18}k_{\text{bridge}}$ of 1.0067 is reduced by the inverse effect from protonation, and $^{18}k_{\text{nonbridge}}$ (1.0069) moves in the normal direction as a result of deprotonation at this site. In summary, the KIE results support earlier proposals of similar transition states between phosphate and sulfate monoester solvolysis. The mechanism is concerted, but the transition state is loose, with little nucleophilic participation, near

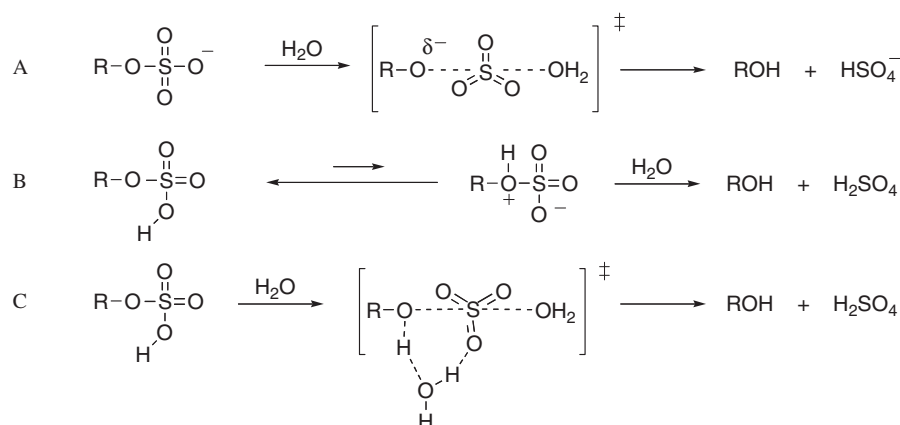


Figure 8 Mechanisms for the hydrolysis of sulfate ester as the anion (A) and as the neutral species (B) and (C). Proton transfer to the leaving group in the reaction of the neutral species may occur in a pre-equilibrium or concerted with leaving group departure.

complete fission of the leaving group bond, and a sulfur trioxide-like center.

The ^{34}S KIE has been measured for the acid-catalyzed hydrolysis reactions of *p*NPS (1.0154) and *p*-acetyl sulfate (1.0172).⁷⁵ Both values are close to estimates for the upper limits of a sulfur isotope effect. For reasons covered earlier in the discussion of central carbon KIEs in acyl transfer reactions, this KIE may be large regardless of mechanism, and only future results will reveal how useful this sulfur isotope effect may be in diagnosing associative from dissociative mechanisms.

KIEs have been measured for the estrogen sulfotransferase-catalyzed sulfonyl transfer from *p*NPS to the 5' phosphoryl group of 3-phosphoadenosine 5'-phosphate (PAP).⁷⁷ The $^{18}(\text{V}/\text{K})_{\text{bridge}}$ of 1.028 is close to the maximum value of this isotope effect and not only indicates advanced bond fission but also demonstrates that the chemistry of sulfonyl transfer is rate limiting. The $^{15}(\text{V}/\text{K})$ of 1.0013 is consistent with only half of a negative charge on the leaving group, suggesting that a residue on the enzyme donates a proton to facilitate leaving group cleavage, but that proton transfer lags behind S–O bond fission. The small normal $^{18}(\text{V}/\text{K})_{\text{nonbridge}}$ (1.0016) is an evidence for a slightly more associative transition state than in the uncatalyzed hydrolysis. Comparison of data for enzymatic and uncatalyzed sulfonyl transfer reactions suggest that the transition states of both are dominated by leaving group bond fission with little to modest nucleophilic involvement.

Sulfate diesters. When a sulfate diester is dialkyl, or aryloxy-alkyl, hydrolysis typically proceeds via alkyl–O bond fission. In the hydrolysis of diaryloxy diesters, an S–O bond cleaves, an assertion that was supported by the incorporation of ^{18}O from solvent exclusively in the

sulfonyl group of the product and none in the phenolic leaving group.⁷⁶ An LFER study found a β_{lg} of -0.7 , a Leffler α_{fission} parameter value of 0.36, and a large negative entropy of activation ($-50 \text{ J mol}^{-1} \text{ deg}^{-1}$). While the β_{lg} suggests substantial change in the effective charge on the leaving group, the small $^{18}k_{\text{bridge}}$ (1.003) does not support significant bond fission. This seeming inconsistency between the β_{lg} and KIEs can be explained by a highly associative transition state, in which the sulfonyl group accepts electron density as the nucleophile attacks. The loss of the sulfonyl group pi bonding will render this group less electrophilic, reducing the effective charge on the aryloxy groups.

Summary

The use of isotopes in many different types of experiments has contributed in fundamental ways to our understanding of the mechanism of reactions of acyl, phosphoryl, and sulfonyl esters. This review cannot do justice to the many scientists who have contributed to such a wide field; it is certain that the use of isotopes will continue to yield insights into the chemistry and biochemistry of esters.

Acknowledgements

Work reviewed in this article from the ACH laboratory has been supported by grants from the NIH (GM47297) and PRF (35690-AC4).

REFERENCES

- Bennet AJ, Brown RS. Physical organic chemistry of acyl transfer reactions. In *Comprehensive Biological Catalysis: A Mechanistic Reference*, vol. 1,

- Sinnott M (ed.). Academic Press: New York, 1997; 293–326; Brown RS, Bennet AJ, SlebockaTilk H. *Accounts Chem Res* 1992; **25**: 481–488.
2. Hengge AC. Transfer of the PO_3^{2-} group. In *Comprehensive Biological Catalysis: A Mechanistic Reference*, vol. 1. Sinnott M (ed.). Academic Press: San Diego, CA, 1998; 517–542.
 3. Hengge AC. *Adv Phys Org Chem* 2005; **40**: 49–108; Thatcher GRJ, Kluger R. *Adv Phys Org Chem* 1989; **25**: 99–265.
 4. Chapman E, Best MD, Hanson SR, Wong CH. *Angew Chem, Int Ed Engl* 2004; **43**: 3526–3548; Lowe G. S^{VI} : sulfotransferases. In *Comprehensive Biological Catalysis: A Mechanistic Reference*, vol. 1. Sinnott M (ed.). Academic Press: San Diego, CA, 1998; 627–635.
 5. Kresge AJ. *Pure Appl Chem* 1964; **8**: 243; Quinn DM. Theory and practice of solvent isotope effects. In *Isotope Effects in Chemistry and Biology*, Kohen A, Limbach H-H (eds). Taylor & Francis: New York, 2006; 995–1018; Schowen KB, Schowen RL. *Methods Enzymol* 1982; **87C**: 551–606.
 6. Marlier JF. *Acc Chem Res* 2001; **34**: 283–290.
 7. Northrop DB. Determining the absolute magnitude of hydrogen isotope effects. In *Isotope Effects on Enzyme-Catalyzed Reactions*, Cleland WW, O'Leary MH, Northrop DB (eds). University Park Press: Baltimore, MD, 1977; 122–152.
 8. Melander L, Saunders WH. *Reaction Rates of Isotopic Molecules*. Robert E. Krieger: Malabar, FL, 1987.
 9. Rishavy MA, Cleland WW. *Can J Chem* 1999; **77**: 967–977.
 10. Parkin DW. Methods for the determination of competitive and noncompetitive kinetic isotope effects. In *Enzyme Mechanism from Isotope Effects*, Cook PF (ed.). CRC Press: Boca Raton, FL, 1991; 269–290; Singleton DA, Thomas AA. *J Am Chem Soc* 1995; **117**: 9357–9358.
 11. Kiick DM. Use of the stable isotope remote label technique to determine isotope effects in enzyme-catalyzed reactions. In *Enzyme Mechanism from Isotope Effects*, Cook PF (ed.). CRC Press: Boca Raton, FL, 1991; 313–330.
 12. O'Leary MH, Marlier JF. *J Am Chem Soc* 1979; **101**: 3300–3306.
 13. Bender ML. *Chem Rev* 1960; **60**: 53–113; Shain SA, Kirsch JF. *J Am Chem Soc* 1968; **90**: 5848–5854; Johnson SL. *Adv Phys Org Chem* 1967; **5**: 237–330; O'Connor CJ. *Q Rev Chem Soc* 1971; **24**: 553–564; Jencks WP. *Chem Rev* 1972; **72**: 705–718.
 14. Bender ML, Dewey RS. *J Am Chem Soc* 1956; **78**: 317–319; Polanyi M, Szabo AL. *Trans Faraday Soc* 1934; **30**: 508–512.
 15. Bentley TW, Carter GE, Harris HC. *J Chem Soc Perkin Trans 2* 1985; 983–990; Bentley TW, Koo S. *J Chem Soc Perkin Trans 2* 1989; 1385–1392.
 16. Kellogg BA, Tse JE, Brown RS. *J Am Chem Soc* 1995; **117**: 1731–1735.
 17. Sawyer CB, Kirsch JF. *J Am Chem Soc* 1973; **95**: 7375–7381.
 18. Bilkadi Z, de Lorimier R, Kirsch JF. *J Am Chem Soc* 1975; **97**: 4317–4322.
 19. Kirsch JF. Secondary kinetic isotope effects. In *Isotope Effects on Enzyme-Catalyzed Reactions*, Cleland WW, O'Leary MH, Northrop DB (eds). University Park Press: Baltimore, MD, 1977; 100–121.
 20. Marlier JF. *J Am Chem Soc* 1993; **115**: 5953–5956.
 21. Stefanidis D, Jencks WP. *J Am Chem Soc* 1993; **115**: 6045–6050.
 22. Marlier JF, O'Leary MH. *J Org Chem* 1981; **46**: 2175–2177.
 23. Satterthwait AC, Jencks WP. *J Am Chem Soc* 1974; **96**: 7018–7031.
 24. Marlier JF, Haptonstall BA, Johnson AJ, Sacksteder KA. *J Am Chem Soc* 1997; **119**: 8838–8842.
 25. Ba-Saif S, Colthurst M, Waring MA, Williams A. *J Chem Soc Perkin Trans 2* 1991; 1901–1908; Ba-Saif S, Luthra AK, Williams A. *J Am Chem Soc* 1987; **109**: 6362–6368; Ba-Saif S, Luthra AK, Williams A. *J Am Chem Soc* 1989; **111**: 2647–2652; Stefanidis D, Cho S, Dhe-Paganon S, Jencks WP. *J Am Chem Soc* 1993; **115**: 1650–1656.
 26. Guthrie JP. *J Am Chem Soc* 1991; **113**: 6045–6050; Tantillo DJ, Houk KN. *J Org Chem* 1999; **64**: 3066–3076.
 27. Xie D, Zhou Y, Xu D, Guo H. *Org Lett* 2005; **7**: 2093–2095.
 28. Buncl E, Um IH, Hoz S. *J Am Chem Soc* 1989; **111**: 971–975; Kwon DS, Lee GJ, Um IH. *Bull Korean Chem Soc* 1990; **11**: 262–265.
 29. Hogg JL, Rodgers J, Kovach I, Schowen RL. *J Am Chem Soc* 1980; **102**: 79–85; Kovach IM, Hogg JL, Raben T, Halbert K, Rodgers J, Schowen RL. *J Am Chem Soc* 1980; **102**: 1991–1999.
 30. Hess RA, Hengge AC. *J Am Chem Soc* 1994; **116**: 11256–11263.
 31. Hess RA, Hengge AC, Cleland WW. *J Am Chem Soc* 1998; **120**: 2703–2709.
 32. Biechler S, Taft Jr RW. *J Am Chem Soc* 1957; **79**: 4927–4935; Schowen RL, Jayarmann H, Kershner L. *J Am Chem Soc* 1966; **88**: 3373–3375.
 33. Marlier JF, Dopke NC, Johnstone KR, Wirdzig TJ. *J Am Chem Soc* 1999; **121**: 4356–4363.
 34. SlebockaTilk H, Rescorla CG, Shirin S, Bennet AJ, Brown RS. *J Am Chem Soc* 1997; **119**: 10969–10975.

35. Slebocka-Tilk H, Neverov AA, Brown RS. *J Am Chem Soc* 2003; **125**: 1851–1858.
36. Stein RL, Fujihara H, Quinn DM, Fischer G, Kullertz G, Barth A, Schowen RL. *J Am Chem Soc* 1984; **106**: 1457–1461.
37. Slebocka-Tilk H, Sauriol F, Monette M, Brown RS. *Can J Chem* 2002; **80**: 1343–1350.
38. Hengge AC, Stein RL. *Biochemistry* 2004; **43**: 742–747.
39. Huskey WP. Origin and interpretations of heavy-atom isotope effects. In *Enzyme Mechanism From Isotope Effects*, Cook PF (ed.). CRC Press: Boca Raton, FL, 1991; 37–72.
40. Melander L, Saunders WH. Secondary hydrogen isotope effects: α -deuterium. In *Reaction Rates of Isotopic Molecules*. Wiley: New York, 1980; 172–174.
41. Abott SJ, Jones SR, Weinman SA, Bockhoff FM, McLafferty FW, Knowles JR. *J Am Chem Soc* 1979; **101**: 4323–4332; Cullis PM, Lowe G. *J Chem Soc Chem Commun* 1978; 512–514; Cullis PM, Lowe G. *J Chem Soc Perkin Trans 1* 1981; **1**: 2317–2321.
42. Arnold JRP, Bethell RC, Lowe G. *Bioorg Chem* 1987; **15**: 250–261; Cullis PM, Iagrossi A. *J Am Chem Soc* 1986; **108**: 7870–7871; Richard JP, Prasher DC, Ives DH, Frey PA. *J Biol Chem* 1979; **254**: 4339–4341.
43. Kirby AJ, Varvoglis AG. *J Am Chem Soc* 1967; **89**: 415–423.
44. Herschlag D, Jencks WP. *J Am Chem Soc* 1989; **111**: 7579–7586.
45. Hengge AC. *Acc Chem Res* 2002; **35**: 105–112.
46. Gorenstein DG, Lee Y-G, Kar D. *J Am Chem Soc* 1977; **99**: 2264–2267.
47. Hengge AC, Edens WA, Elsing H. *J Am Chem Soc* 1994; **116**: 5045–5049.
48. Khan SA, Kirby AJ. *J Chem Soc (B)* 1970; 1172–1182.
49. Kirby AJ, Younas M. *J Chem Soc (B)* 1970; 510–513.
50. Cleland WW, Hengge AC. *FASEB J* 1995; **9**: 1585–1594.
51. Cassano AG, Anderson VE, Harris ME. *J Am Chem Soc* 2002; **124**: 10964–10965.
52. Hall CR, Inch TD. *Tetrahedron* 1980; **36**: 2059–2095.
53. Anderson MA, Shim H, Raushel FM, Cleland WW. *J Am Chem Soc* 2001; **123**: 9246–9253.
54. Catrina I, O'Brien PJ, Purcell J, Nikolic-Hughes I, Zalatan JG, Hengge AC, Herschlag D. *J Am Chem Soc* 2007; **129**: 5760–5765.
55. Zhang Z-Y. *CRC Crit Rev Biochem Mol Biol* 1998; **33**: 1–52.
56. Fauman EB, Yuvaniyama C, Schubert H, Stuckey JA, Saper MA. *J Biol Chem* 1996; **271**: 18780–18788; Stuckey JA, Schubert HL, Fauman EB, Zhang Z-Y, Dixon JE, Saper MA. *Nature* 1994; **370**: 571–575.
57. Hengge AC, Sowa GA, Wu L, Zhang Z-Y. *Biochemistry* 1995; **34**: 13982–13987.
58. Hengge AC, Denu JM, Dixon JE. *Biochemistry* 1996; **35**: 7084–7092.
59. Hengge AC, Zhao Y, Wu L, Zhang Z-Y. *Biochemistry* 1997; **36**: 7928–7936.
60. Rusnak F, Mertz P. *Physiol Rev* 2000; **80**: 1483–1521.
61. Hengge AC, Martin BL. *Biochemistry* 1997; **36**: 10185–10191.
62. Martin B, Pallen C, Wang J, Graves D. *J Biol Chem* 1985; **260**: 14932–14937.
63. Mertz P, Yu L, Sikkink R, Rusnak F. *J Biol Chem* 1997; **272**: 21296–21302; Hoff RH, Mertz P, Rusnak F, Hengge AC. *J Am Chem Soc* 1999; **121**: 6382–6390.
64. Raushel FM. *Curr Opin Microbiol* 2002; **5**: 288–295.
65. Vanhooke JL, Benning MM, Raushel FM, Holden HM. *Biochemistry* 1996; **35**: 6020–6025.
66. Lewis VE, Donarski WJ, Wild JR, Raushel FM. *Biochemistry* 1988; **27**: 1591–1597.
67. Caldwell SR, Newcomb JR, Schlecht KA, Raushel FM. *Biochemistry* 1991; **30**: 7438–7444.
68. Caldwell SR, Raushel FM, Weiss PM, Cleland WW. *Biochemistry* 1991; **30**: 7444–7450.
69. Benkovic SJ, Benkovic PA. *J Am Chem Soc* 1966; **88**: 5504–5511.
70. Garner HK, Lucas HJ. *J Am Chem Soc* 1950; **72**: 5497–5501; Kaiser ET, Panar M, Westheimer FH. *J Am Chem Soc* 1963; **85**: 602–607.
71. Fendler EJ, Fendler JH. *J Org Chem* 1968; **33**: 3852–3859.
72. Chai CLL, Hepburn TW, Lowe G. *J Chem Soc, Chem Commun* 1991; **19**: 1403–1405.
73. Kice JL, Anderson JM. *J Am Chem Soc* 1966; **88**: 5242–5245.
74. Hoff RH, Larsen P, Hengge AC. *J Am Chem Soc* 2001; **123**: 9338–9344.
75. Burlingham BT, Pratt LM, Davidson ER, Shiner VJJ, Fong J, Widlanski TS. *J Am Chem Soc* 2003; **125**: 13036–13037.
76. Younker JM, Hengge AC. *J Org Chem* 2004; **69**: 9043–9048.
77. Hoff RH, Czyryca PG, Sun M, Leyh TS, Hengge AC. *J Biol Chem* 2006; **281**: 30645–30649.